Off-Axis Response of Limb Emission Sensors Derived from Lunar Scans

Larry L. Gordley & Yunfei Wang
GATS,Inc., Newport News, VA

James Russell,III
Hampton University, Hampton, VA

M.G.Mlynczak
NASA Langley Research Center, Hampton, VA

Abstract:

Deriving atmospheric state parameters from Earth limb emission demands accurate knowledge of off-axis response. Sounding the upper atmosphere (>60km) can require knowledge of the off-axis(>1.0 degrees from on-axis) to an accuracy of 10^{-5} or better, relative to on-axis. This level of sensitivity is very difficult and expensive to achieve in the laboratory. We describe the use of lunar scans to determine the off-axis response of the SABER (Sounding of the Atmosphere using Broadband Emission Radiometry) instrument on-board the NASA TIMED (Thermosphere, Ionosphere, Mesosphere Energy and Dynamics) satellite. SABER is a 10-channel emission sensor that performs high resolution scans of the Earth limb for studies of the mesosphere and thermosphere. The off-axis calibration method bootstraps from the precise on-axis FOV measured in the laboratory, by characterizing the lunar source function, which is then used to infer the very weak distant low-resolution off-axis response. Procedures and results are presented.

Introduction

The Moon which has a diameter about 32 minutes of are (about 0.5 degrees) has been

used as a post-launch calibration target for many instruments on Earth-orbiting spacecraft for many years[1-8]. The use of lunar observations includes monitoring solar bands radiometric stability, deriving correction parameters, characterize the electronic crosstalk under different focal plane operational configurations, tracking on orbit band to band registration. The lunar view has also been used to validate the accuracy of sensor efficiency, FOV and LOS for instruments with FOV many times larger than the diameter of the moon (about 0.5 degrees). To our knowledge, the concept of this paper (to derive off-axis response of limb emission sensors from lunar scans) has not been described in any other studies. The objective of this study is to verify/generate the far off axis section of field of view (FOV) functions across all of SABER's detectors across the focal plane.

SABER Instrumentation

SABER instrument has 10 channels on the focal plane that will measure atmospheric emissions in the 1 to 17 micro meter spectral range. Each detector has an instantaneous field of view (IFOV) of 0.7 mrad by 10 mrad. Detailed descriptions of instrument are available eleswhere.[9-11] The size of the detectors on the focal plane and the size of the moon relative to the sensors are illustrated in Figure 1. The nominal FOV scan velocity is 0.179 degree/sec and the nominal sampling rate is 44 msec per sample (22.73 Hz).

The actual FOV has been calibrated pre-launch in the lab using a point source and slit sources. Elevated channel response away from the central IFOV lobe that shows no correlation with another channel's location is observed in addition to channel cross talk. The source of this response has not been identified. However, this should not be real. Figure 2 shows the plot of the dynamic IFOV for each channel measured at tangent altitude of 130km during the ground calibration.

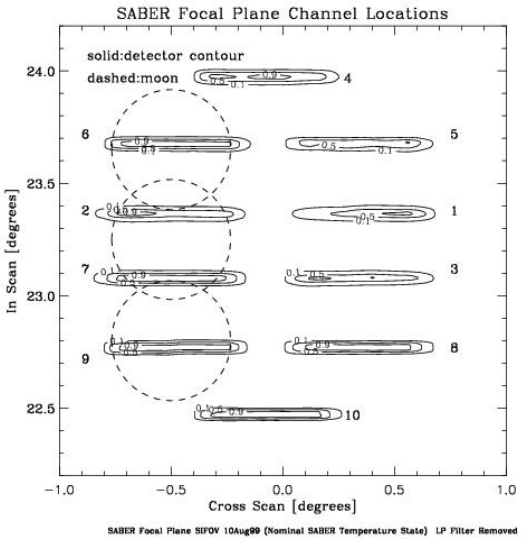

First approach to estimate the off-axis FOV was achieved by combining data from near angle scattering and IFOV measurements. Elevated channel response away from the central peak was replaced by a straight line for every long wave channel as illustrated in the Figure 3.

The Moon was used as a hot source with a cold background in this study. It is assumed that the phase of the moon and the elevation/altitude of the moon changes very slowly. The moon crossed the view of SABER instruments several times this year. Three periods have been investigated in this study. The first one occurred from January 22nd to 24th this year with the moon phase at 67%. The second period was from March 22nd to 24th (moon phase 65%) and the third was from April 16th to 18th (moon phase 99%). Each period has about 20 orbits that contain a lunar scan sequence. When the moon crossed into the SABER's view, the instrument was commanded to conduct short lunar scans at nominal speed of 0.179 degrees/second. It did a sequence of repeated up and down scans over the moon (from about 1.5 degrees above the center of the moon to 1.5 degrees below the center of the moon). Data were recorded at every 44 msec. The situation resembles the FOV measurements using point and slit source in the ground calibration in scan pattern. However, a point source and slit sources were used in the ground calibration. The power spectral remains constant for a FOV ground measurement. The elevation angle of the moon center as function of time has been investigated in this study. For each moon scan sequence, the change of moon elevation angle as function of time (delta angle/delta time) was calculated and the results are very small. For example, orbit 6095, the rate is 0.00427 degrees/minute. For orbit 06971, the rate is 0.002321 degrees/minute.

These results indicate that our assumption on moon movement is reasonable.

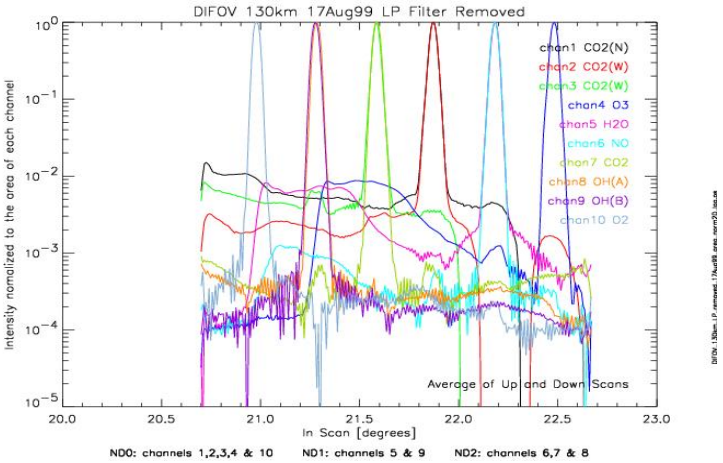

Figure 2. SABER In-Scan IFOV

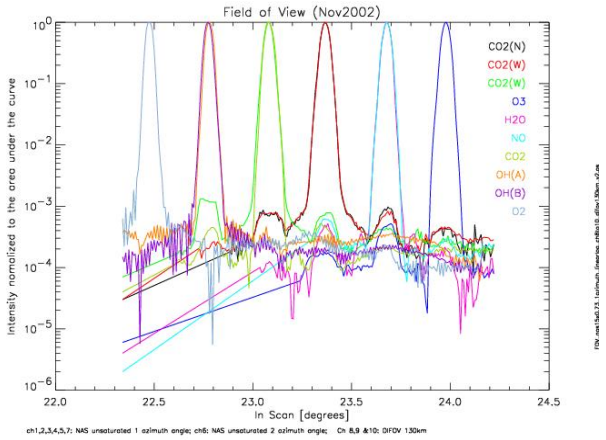

Figure 3. Lab on-axis FOV with guessed off-axis FOV

Processing Techniques and Procedures

Initial SABER Level1B Processing

Processing raw saber data follows established techniques for removal of instrumental effects such as low pass filter, detector bias (offsets), response conversion from (counts) to Watts/(m2*sr) and channel alignment. In the final processing of this step, the radiance profile of each channel was projected onto an uniformed elevation grid (0.4 degree interval). The tangent point location corresponding to the elevation grid was also calculated.

Lunar Observation Analysis of One Lunar Scan Sequence

After the initial processing, the scans with the moon in the field within 3 angular degrees of the sensors line of sight are summed up and averaged over azimuth positions to generate the rising radiance profile of the moon region. On the other hand, the sum of low radiance profiles before and after the moon entered and left the sensor FOV are averaged to generate a good reference profile corresponding to a offset without the moon in the FOV. This reference profile was then subtracted from the moon radiance profile to obtain the "real" moon profile. This step minimized the impact of slight drifts in the sensor zero-radiance offset. Figure 4 illustrated a lunar profile generated using this algorithm. Finally, the center elevation angle of each channel was located by using the 50% integrated area and the moon radiance profile are registered on uniformed elevation angle grid referenced to the center of the moon for each channel. The altitude above the moon will have positive elevation angle values.

Summing up all processed valid normalized lunar profiles

In this study, we used only orbits that have lunar scan sequence in which (1) the lunar image passed within 3 degrees of the line of sight from the center of the focal plane, and in which (2) good reference radiance of space were available before and after the lunar radiance measurements. There were 20 orbits used for January,2003. It is assumed that The summing of a large amount of azimuth position is equivalent to the convolution of the one dimension moon over the one dimensional FOV. This assumption can be proved under simplified conditions. Assume that the 2D moon is a circle with a diameter of 32 minutes of arc and the 2D SABER FOV is a rectangular with the length of 10 mrad and width of 0.7 mrad. If the intensity of the moon and the FOV are both uniformly distributed, The convolution of 2D moon over the 2D FOV for a large number of azimuth positions is equivalent to the convolution of the 1D moon (summed across azimuth angles) over the 1D FOV.

Correct channel saturation

In our study, channel saturation occurred for channels 4 to 10 in various degrees. This problem was estimated and minimized by taking the FOV of channel2 (unsaturated CO2 wide channel) and replace the center of channels 4-10 with the center of channel 2 by fitting (scaling and aligning) the sides on the channel 2 FOV to the channel n FOV(n=4 - 10). The resulting area was then normalized to lab FOV center area. The next figure (Figure 5) illustrates the result of this step for SABER O3 channel.

Derive the final FOV using lab derived FOV and the lunar derived FOV

This final step is illustrated in Figure 6. The convolution of lunar FOV(center lobe, red curve) over lab guessed FOV (black curve) was calculated and the new final FOV was generated by multiplying the lab measured FOV by the ratio of the lunar derived FOV divided by the lunar (center) convolved FOV and replace old far off axis FOV values with new values. The blue curve represents the final FOV for channel 4 in Figure 6.

To verify this technique used in this final step, a bias of 1.e-4 was introduced to the final FOV (the blue curve in Figure 6, assuming this is the true FOV) to generate a faulty FOV (see the illustration in Figure 7). Then convolve the moon central lobe over the “true” and faulty FOV respectively to obtain the green curve and blue curve in Figure 7. Finally, multiply the faulty FOV by the ratio of Ltrue/Lfaulty and compare it to the “true” FOV. The resulting curve (red curve) shows that this method does bring the faulty FOV back to the true FOV level at far off-axis.

Results and Discussions

The FOV (lab and lunar (Jan,2003) derived FOV of all ten channels are illustrated in Figure 8. Fig 9 shows how the off-axis FOV changed from the original lab measurements to lab guessed and finally to the lunar derived FOV.

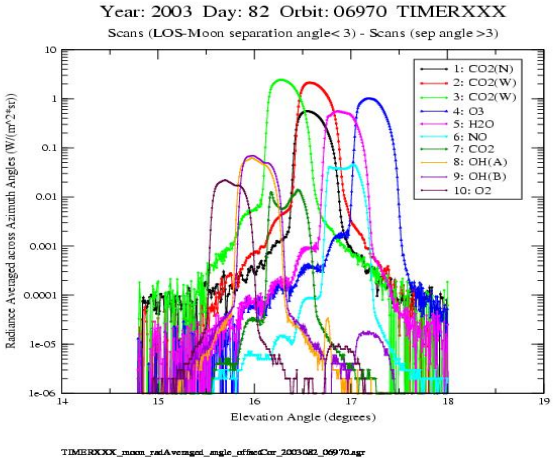

Figure 4. Lunar Scan of One Orbit

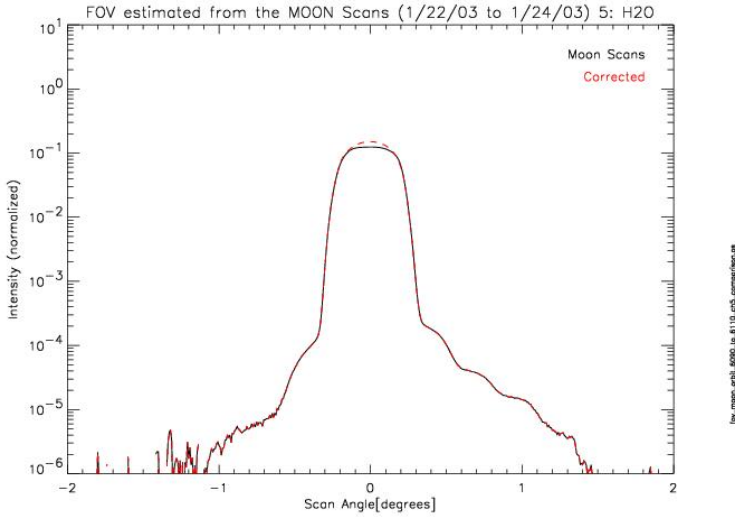

Figure 5. Channel Saturation in Lunar Observation

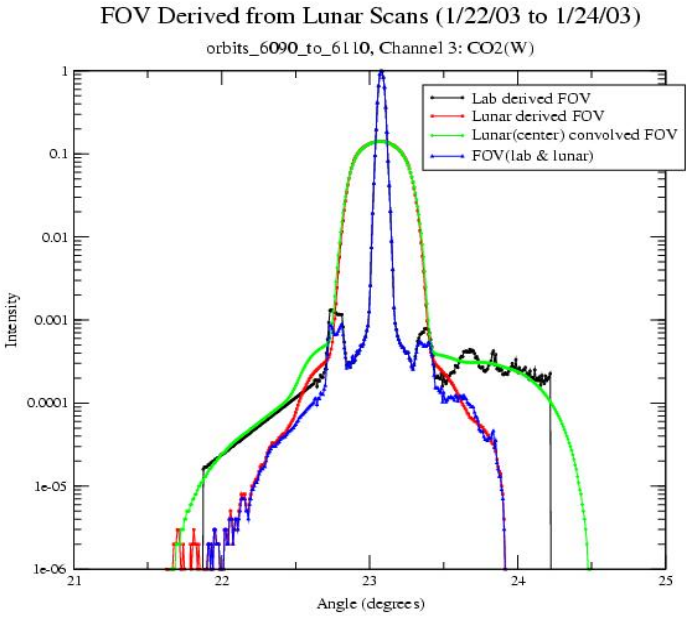

Figure 6. FOV Derived from Lunar Scans

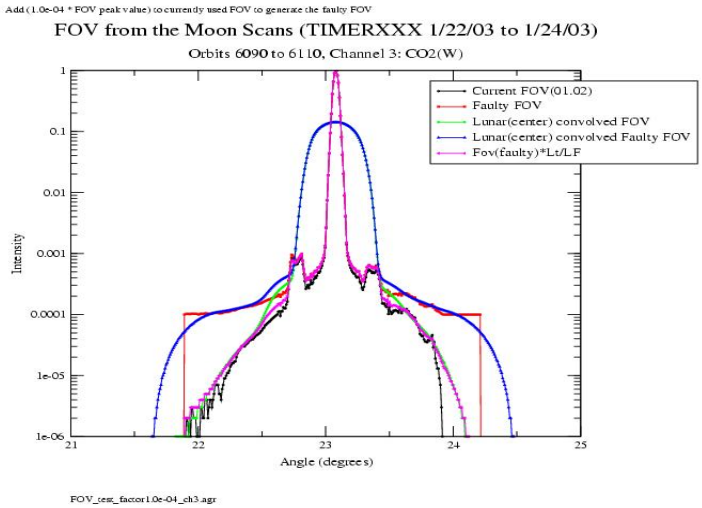

Figure 7. Illustration of retrieving “true” FOV from a “faulty” FOV

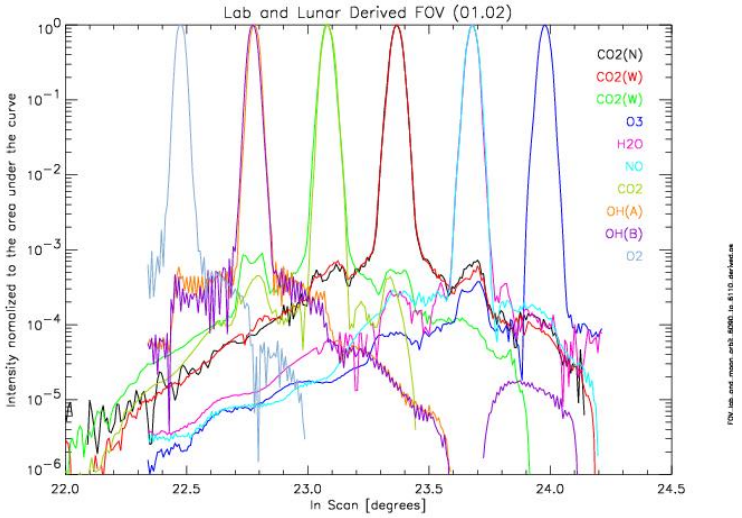

Figure 8 Lab and Lunar Derived FOV

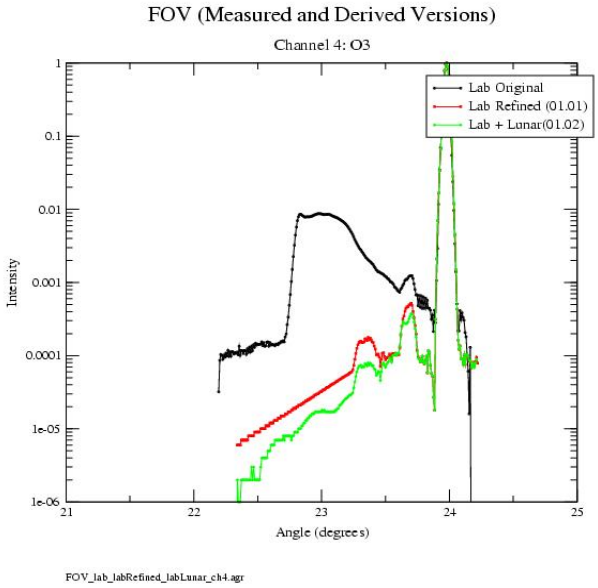

Figure 9. Comparison of lab measured FOV, lab refined FOV and lunar derived FOV

Results of lunar derived FOV from 3 periods are plotted in Figure 10. It is observed that despite the moon phase differences (65% to 99% phase), the off-axis FOVs are very similar for all three periods.

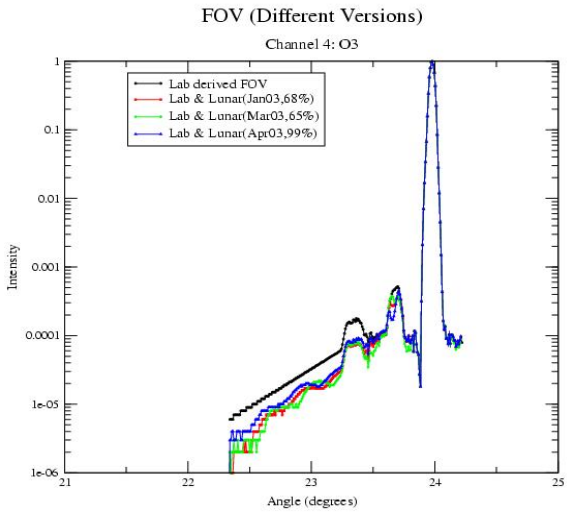

Figure 10. Comparison of lunar derived FOV from three lunar observation periods

The uncertainty of the final FOV was estimated by differencing the FOV derived from 65% phase and the 99% phase. The absolute values of the difference as function of elevation angles are the uncertainties illustrated in Figure11 for channel 4 (O3).

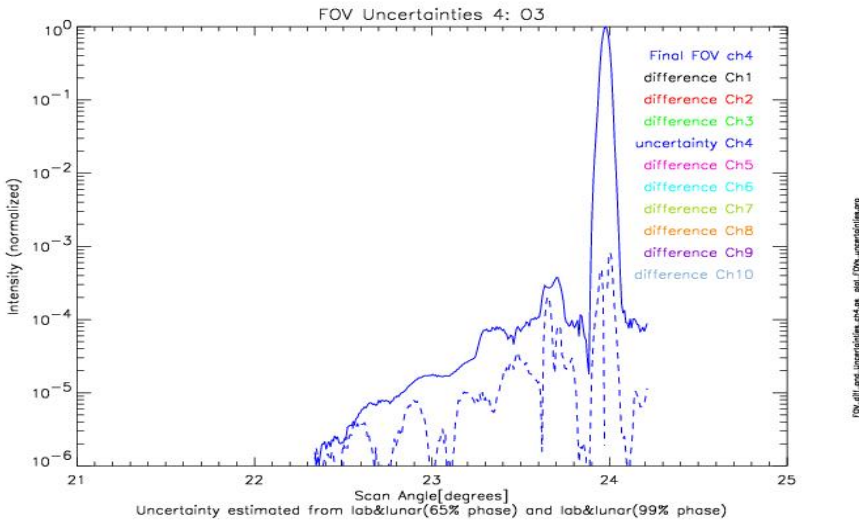

Figure 11. Uncertainty of lunar FOV

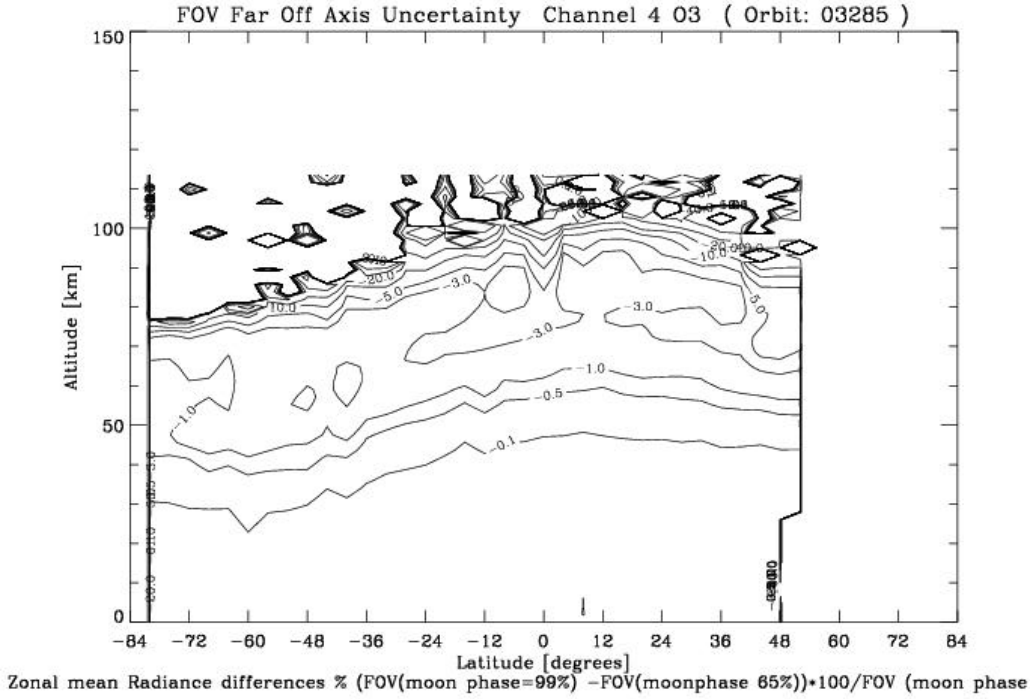

Figure 12. Zonal mean radiance uncertainty from FOV uncertainty

The radiance uncertainty was also estimated from radiance determined using FOV derived from moon phase 65% and the radiance determined using FOV derived from moon phase 99% and the zonal mean results are shown in the Figure 12.

Summary

We developed a data collection and analysis process to derive and validate far off-axis FOV using the moon observations. The lunar functions can be accurately calibrated using a large statistical set of lunar scans since they are only varying in angle slowly. The calibration of these functions requires only relative response, therefore uniformity or absolution knowledge of lunar emission is unnecessary. This study has demonstrated the optical performance of the SABER instrument, giving confidence to the measurement analysis and altitude resolution.

References

1. H.H.Kieffer, and J.M.Anderson, “Use of the moon for spacecraft calibration over 350-2500 nm”, Proc. Of SPIE, 3498,325-336,1988.
2. R.A.Barnes, R.E.Eplee,Jr. and F.S.Patt, “SeaWiFS Measurements of the Moon”, Proc. SPIE 3438,311-324,1988.
3. R.A. Barnes, R.E.Eplee, F.E. Patt and C.R. McChain, “Changes in the radiometric response of SeaWiFS determined from lunar and solar-based measurements”, Applied Optics 38, 4649-4664 ,1999.
4. Thomas C. Stone and Hugh H. Kieffer, “Absolute irradiance of the moon for on-orbit calibration”, Proc.SPIE, 4814, 211-221, Seattle, WA, 2002.
5. X.Xiong, J.Sun, K.Chiang, S.Xiong and W.L. Barnes, “MODIS on-orbit characterization using the Moon”, Proc. SPIE 4881, 299-307,2003.
6. J.Sun, X.Xiong, B.Guenther and W.barnes, Radiometric stability monitoring of the MODIS reflective solar bands using the Moon”, Metrologia 40, S85-S88,2003.
7. K.Shiomi, A.Yamazaki, I.Yoshikawa, Y.Takizawa, and M.Nakamura, “Post-launch Calibration of the Planet-B Extreme Ultraviolet Scanner”, Lunar and Planetary Science,XXXIV,1207,2003
8. R.B.Lee III, G.L.Smith, D.P. Kratz, K.J. Priestley, Z.P. Szewczyk, S.Thomas, K.A. Bush, J.Paden, D.K.Pandey, R.S. Wilson, and A.Al-Hajjah,“Measurements of filtered lunar radiances using the NASA Terra spacecraft/CERES thermistor bolometer sensors during 2000 and 2001”,Proc of SPIE,5151,2003.
9. SDL/95-009,1999, SABER instrument specification (Space Dynamics Laboratory).
10. SDL/95-006,1998, SABER instrument requirements document.
11. Tansock, J.J., S. Hansen, K.paskett, A.Shumway, J.Peterson, J.stauder, L.Gordley, Y. Wang, M. Melbert, J.Russel, and M.G. Mlynczak,”SABER Ground Calibration”, Int. J. Remote Sens., 24, 403-420,2003.